JOURNAL OF OPTOELECTRONICS AND ADVANCED MATERIALS Vol. 10, No. 1, January 2008, p. 29 - 43

*Review Paper*

# Nonlinear optical effects in new alkynyl-ruthenium containing nanocomposites

J. LUC, A. MIGALSKA-ZALAS[a,*], S. TKACZYK[a], J. ANDRIÈS[b], J-L. FILLAUT[b], A. MEGHEA[c], B. SAHRAOUI
*Laboratory POMA, University of Angers, UMR CNRS 6136, 2 boulevard Lavoisier, 49045 Angers Cedex 1, France*
*[a]Institute of Physics, J. Dlugosz Academy of Czestochowa, PL-42217, Aleja Armii Krajowej 13/15, Czestochowa, Poland*
*[b]Sciences Chimiques, University of Rennes 1, UMR CNRS 6226, Campus of Beaulieu, 35042 Rennes Cedex, Franc*
*[c]Applied Spectroscopy Laboratory Department of Applied Physical Chemistry and Electrochemistry, Faculty of Industrial Chemistry, «Politehnica» University of Bucharest, Romania*

A theoretical and experimental study of third-order nonlinear optical properties of alkynyl-ruthenium complexes bearing terminal hydrogen-bonding receptors are presented. These materials could be promising materials for the molecular engineering for applications in organometallic chemistry and nonlinear optics. We have obtained the third-order nonlinear optical susceptibility $\chi^{<3>}$ for each studied complex. A good agreement between the proposed theoretical model and the experimental results was found. The investigated complexes show large optical nonlinearities in comparison with $CS_2$, which is the reference material for DFWM measurements. The data obtained through the theoretical study provide valuable insight into the origin of the hyperpolarizability and help to synthesize molecules with optimal properties, which are important for nonlinear optics and molecular engineering.

(Received in the last form January 8, 2007; accepted January 12, 2007)

*Keywords*: Third-order optical susceptibilities, Degenerate four wave mixing, Alkynyl-ruthenium complexes, Quantum chemical calculations, Second-order molecular hyperpolarizabillity

## 1. Introduction

The application of nonlinear optical devices in telecommunication requires novel materials with optimized nonlinear susceptibilities. In the recent years, there has been considerable progress in designing and characterizing molecular organometallic systems with strong second and third order optical nonlinearities. Due to their efficiency, chemical flexibility and high conjugated framework, organometallic complexes have received particular attention as new materials for NLO [1].

We report the measurements of the third-order nonlinear optical susceptibilities of new alkynyl-ruthenium complexes bearing terminal barbituric based electron withdrawing heads, by using the degenerate four wave mixing (DFWM) technique in picosecond regime (at $\lambda$ = 532 nm). From these measurements, we deduced the values of second-order hyperpolarizabilities $\gamma$, which are about $10^4$ larger than the $\gamma$ value of $CS_2$. We determined also the values of third-order nonlinear optical susceptibilities for various polarizations of incident beams and their corresponding molecular and electronic contributions. We showed the influence of several $\pi$-conjugated transmitters on nonlinear optical properties of the resulting push-pull systems. A study on the optimal molar concentration and the temporal coherence of incident beams allowed optimizing the DFWM efficiency for the studied alkynyl-ruthenium complexes.

The present study is a natural continuation of our previous work concerning the analysis of nonlinear optical properties of other families of alkynyl-ruthenium complexes [2-4]. In this paper, we report the results obtained in the NLO characterization of a novel series of donor-transmitter-acceptor alkynyl ruthenium chromophores incorporated in dichloromethane solvent and in a polymethyl methacrylate (PMMA) polymer matrix. The third-order nonlinear optical susceptibilities of these solutions were measured by the degenerate four wave mixing (DFWM) technique [**5**]. The properties of third-order nonlinear optical properties were carried out for a fundamental wavelength at 532 nm from a Nd:YAG laser with a pulse duration of 30 ps, at the repetition rate frequency of 1 Hz. This new family of alkynyl-ruthenium complexes reveals very interesting properties for NLO applications.

In this work, we also present the theoretical quantum chemical calculation of a second-order molecular hyperpolarizability of the mentioned organometallic molecules. The proposed theoretical approach rely on geometry optimisation and corresponding quantum chemical calculations based on semi-empirical ZINDO/1 method within a framework of the restricted Hartree-Fock approach. The quantum chemical calculations give

important information concerning the origin of the observed spectra and information for desirable changes of the chemical content using appropriate substitution. A substitution of the different groups at the end of backside group causes the substantial changes of both absorption spectra as well as nonlinear optical parameters. Comparison of theoretical results with the experimental data is presented.

## 2. Organometallic complexes

An organometallic complex can be defined as a chemical compound comprising at least a carbon-metal bond. The incorporation of transition metals (a metal is known as of transition if it has an incomplete $d$ electronic orbital in one of its states of oxidation) is important in creating functional materials (linear and nonlinear optical, luminescence, electron transport, etc as the metal center very deeply modifies the electronic properties of the organic counterpart. For instance, this may result in important modifications of the reactivity of this organic part, one of the most successful application being homogeneous catalysis using transition metal based catalysts. A increasing number of the latter materials should be of particular interst to industrial chemists.

The dimethylarsanyl oxide ($(CH_3)_2As)_2O$ can be considered as the first organometallic complexe to be synthesized, and was first prepared by Cadet in 1760. Its structure was finally elucidated by Bunsen, in 1843. One second family of organometallics, a platinum olefin complex, was developed more tardily in 1827 by Zeise. Later in 1900, with the development of the organomagnesium compounds by Barber then Grignard, started a true metamorphosis of the organic synthesis. However, it is necessary to await 1951 and the discovery of ferrocene and the rationalization of its sandwich structure by Wilkinson and Woodward [**6**] so that the organometallic chemistry of transition metals took its rise.

### 2.1. Monometallic complexes

Transition metals are, by definition, elements with incomplete orbitals and their last orbital $p$ is empty. To give place to the existence of stable compounds, these elements will have more or less to supplement these underorbitals of valence by electrons given or shared by the ligands. These electrons brought by the ligands thus make it possible the transition metal to reach, or at least to border, the electronic structure of the rare gas which follows it on the same line of the periodic table [7].

There are primarily two types of ligands:

- those which bring one or more pairs of electrons to metal, i.e. the ligands L or $L_n$ noted "even" (n being the number of pairs of electrons given to metal),
- those bringing an odd number of electrons to metal, i.e. the ridicalizing ligands noted X (an electron) or $L_nX$ (an odd number of electrons).

Whereas a ligand L or $L_n$ formally does not take any electron with metal to form the metal-ligand bond since it acts of a donor-acceptor bond, the ligand X or $L_nX$ shares the bond with metal by requiring of him an electron as in a covalent bond in organic chemistry.

### 2.2. Applications of organometallic complexes

One of the most famous natural representatives of the organometallic complexes is hemoglobin. Hemoglobin is a molecule present in the red globules of blood. It plays a major part in breathing: at the time of its passage in our lungs, it collects oxygen and then distributes it in the whole of our body. The structure of this protein is known today: it consists of four monomers of globulines and four molecules of heme containing each one an iron atom protected by organic molecules which confer its properties to him. The observations confirm that when iron is associated at the protein, this one becomes active in the transport reaction of oxygen: the role of metal is thus dominating.

The organometallic compounds are well known for their application in complex multistep synthesis and as catalysts in various chemical reactions. For more than 50 years, the chemical industry used the organometallic complexes for their catalyst capacities, i.e. their capacity to take part in the transformation of natural products in reactions using a minimum of energy. The part played by the metal part of the complex is major as it is for example the case of some derived from platinum, palladium, ruthenium and other rare metals. The metallocenes (ferrocene being the most popular) are used in certain syntheses of the carbon nanotubes (CNT) using methods of chemical vapor deposition (CVD) [8].

Several environmental aspects can also benefit from the use of organometallic based systems (green chemistry). The phosgene, used formerly as poison gas, is a very toxic reagent containing chlorine and of carbon monoxide and is used today for the agriculture manufacture. The chemists thought of the possibilities to replace in these reactions, the phosgene by the carbon dioxide ($CO_2$) present in superabundance on planet and to use for those organometallic complexes.

Generally, at the time of chemical reactions, the products put in presence can, according to their structure, to carry out electronic transfers. By manufacturing unsaturated organometallic compounds in electrons, it is possible to confer the property to them to react with oxygen. Thus, one can manufacture an oxygen absorber: a capsule containing an organometallic complex is introduced into the packing of a foodstuff which one wishes to put safe from air but nonvacuum. The contents of the capsule will absorb all oxygen in air present in the

envelope and will eliminate the risks of degradation of the product. A second industrial development is the detecting oxygen indicator: placed in the packing of a vacuum put product, a capsule changes color when it is put in contact with the air during a few hours. By a simple glance, the consumer can thus check the sealing of packing.

Molecular electronics involving organometallic compounds is currently widely investigated because of their specific optical, magnetic and electronic properties, including nonlinear properties of organometallics and their potential applications. It is essential to understand the electronic structure of the complexes and the principal modes of bonds between the metals and current ligands. A molecule which absorbs laser light is located in an excited electronic state. Its geometrical structure is modified, its movements of vibration and rotation are more important. The excess of energy brought by the absorbed photon is evacuated several manners: it can be dissipated thermically towards the environment of the molecule, or this one can emit light, or take part in a chemical reaction. Compared with the other chemical species, the photophysics and the photochemistry of the complexes of transition metals are particularly rich and attractive. Indeed, these compounds have a great number of excited electronic states, very close in energy, located in the visible and the near ultraviolet [9]. The denomination of the excited states of the complexes of transition metals is function of the change which they induce in the distribution of the electronic density of the molecule (different charge transfers).

### 2.3. Organometallic complexes in NLO

The interest of the organometallic complexes in NLO comes from their particular electronic capacities in term of charge transfer [10-12]. Indeed, their optical spectra often present intense transitions in visible bringing into play the metal-ligand charge transfer (MLCT) or conversely. In particular, the acetylide organometallic complexes having a linear structure of type M-C≡C-R generate a strong coupling between metal and π-conjugated way and have consequently strong optical non-linearities [13, 14]. Moreover, these π-conjugated chains containing organometallic carbon-rich complexes are interesting materials for the study electron transfer [15-17], liquid crystal formation [18], and for the design of molecular components [19, 20] or for applications in nonlinear optics [21]. Indeed, organized in molecules or polymers, they can become materials having of remarkable nonlinear optical properties. Our work is located in this specific field of research.

The M-C≡C- unit allows the existence of a strong mesomery within the complexes and improves the intramolecular charge transfer between the organometallic group donor and the organic conjugated part that lies in the same plane as this unit. Theoretical and experimental studies on these complexes showed that the strong hyperpolarisability of the second order $\beta$ characterizing the nonlinear optical efficiency of the molecule depends on the length of the π-conjugated way and the force on the groups donor (metal) and acceptor. Moreover, it was observed that the nonlinear response of the second-order increases thanks to the multiple metal-carbon bonds present in this type of complexes [22]. More particularly, beside unidimensional compounds, were also developed complexes of transition metals and multipolar bi- and three-dimensional systems [23-26] such as for example the octupolar systems. Indeed, the tensorial character of second-order non-linearity makes it possible to consider the design of molecules having a higher symmetry that the simple dipolar symmetry.

### 2.4. Organometallic complexes containing ruthenium

Ruthenium, coming from the Latin word *Ruthenia* meaning Russia, is available today commercially (world production of 12 tons per annum or approximately 1 $m^3$). It was identified and insulated in 1844 by Klaus which showed that the ruthenium oxide contained a new metal and extracted six grams of them from the insoluble part of rough platinum in regal water (mixture of three volumes of hydrochloric acid with a volume of nitric acid able to dissolve certain metals). With rhodium, palladium, osmium, iridium, and platinum, it belongs to the "group of platinum". One meets it most of the time in a native state (in the form of silver shining metal and with a hexagonal crystalline structure) or in alloy with platinum. The most important mineral is laurite ($RuS_2$). One also meets ruthenium traces in a series of copper and nickel ores. It is inalterable with the air and practically unattackable by the acids, including regal water, unless adding potassium chlorate. It is known to be used as superconductor or like catalyst in chemistry and also makes it possible to increase the hardness of platinum, palladium and titanium. It is used in many applications, such as for example in the jewels, the feathers of pen, the electrodes of spark plugs, the separators of the magnetic layers of the hard disks of computers ("Pixie-Dust" technology), ...

In periodic classification, it belongs to the family of transition metals (group 8, period 5) and its molecular mass is worth 101.07 $g.mol^{-1}$. Its symbol is "Ru", its atomic number is Z = 44 and its atomic configuration is $[Kr]4d^7 5s^1$. One can find ruthenium under various oxidation states (2, 3, 4, 6 and 8). The energy levels of orbital molecular, formed at the time of its complexation, can be described by a linear combination of atomic orbitals of metal and the molecular orbitals of ligands.

The ruthenium complexes form part of the most studied organometallic compounds for NLO [27-30] because of their synthetic versatility and accessibility, their stability (both chemical and thermal) and the reversibility of the $Ru^{II}/Ru^{III}$ redox couple [31, 32]. In particular, the organometallic complexes ruthenium acetylures represent one of the metal classes of complexes the most studied in the second-order NLO [1, 33]. In these complexes, the metal groups are directly incorporated in the same plan as that of the π-conjugated way, fulfilling thus the requirements of design of push-pull chromophores having strong second harmonic efficiency [34, 35]. Metal acts as a group donor in the push-pull system and the second-order nonlinearity can be related to the excitations of low energy of the MLCT. Moreover, the organometallic complexes of type acetylide metal present good predispositions for the third-order NLO [36]. It was even shown more recently than the existence of a strong electronic delocalization on the π-conjugated way of this type of systems was at the origin of third-order nonlinear phenomena [37, 38]. The acetylide derivatives of ruthenium(II) are among the alkynyls systems most studied in NLO [39], the ruthenium-alkynyl group being a very strong donor which can compete with the strongest organic donors [40, 41]. These properties come indeed mainly from the result of the overlapping between the $d$ orbital of ruthenium and the π-conjugated way and can thus be modified systematically through the variation of the organic π system or the electronic richness of the alkynyl-ruthenium part.

### 2.5. Studied organometallic complexes

The molecules inserting one or more metal centers are currently investigated with increasing interest. The alkynyl organometallic complexes represent one of the series most largely studied metal complexes [18, 42]. The metal-carbon bond and the electronic delocalization through a π-conjugated system towards an acceptor are the criteria of efficiency associated with this design. The criteria evoked in the literature [18, 28, 42] making it possible to tend to a better nonlinear optical efficiency suggest a lengthening of the π-conjugated system connecting the donor group to the acceptor group and impose a multiple bond at the metal-carbon bond of the organometallic group. In this study, we investigated the nonlinear optical properties of a series of alkynyl organometallic complexes $\sigma$ having a common group of alkynyl-ruthenium *trans*[$(dppe)_2$Ru-C≡C-] (dppe = diphenylphosphinoethane) improving the stability of the molecule. The phosphine ligands, electrodonor, are particularly appreciated since they enrich metal in electrons and provide a good stability of the complex in three-dimensional space (steric protection) which directly contributes to make these complexes effective in NLO.

The studied planar push-pull systems have the same donor (the ruthenium alkynyl group) and different transmitters and acceptors. These different configurations suggested enabled us to continue the research of the best compromise for a [Donor-Transmitter-Acceptor] unit and to highlight the influence of the variations in the chemical structure of the studied complexes on third-order optical nonlinearities.

The methods of synthesis employed for the preparation of these ruthenium complexes were adapted starting from procedures reported previously in the reference [43]. The studied organometallic complexes were synthesized in the powder form at a scale from 50 to 100 mg. These organometallic complexes were characterized optically in dichloromethane solvent and were incorporated in polymeric matrices of polymethyl methacrylate (PMMA) in order to study their nonlinear optical properties. These molecules are assimilable to a molecular switch since its topology can completely and be reversibly modified by chemical way (series of reversible protonation/deprotonation on the level of donor and acceptor) or modulated by effects of solvent. Fillaut et *al.* noticed that the alkynyl ruthenium complexes, having an acceptor methylene-barbiturate as it is the case for these complexes, present very flexible electronic properties [44, 45]. Indeed, this type of complexes show a very great sensitivity to nature of solvents and the interaction solution-solvent (solvatochromism) [46] in which they are placed, which results visually in notable changes of the color of the solutions. These materials can act for example as effective anion sensors in nonpolar solvents where they exhibit broad changes of color [43, 47].

The chemical structures of the studied molecules are presented in Fig. 1. For convenience the complexes will be indicated by **a-d**.

In this work, we have studied the effect of π-conjugated transmitter variation and of two types of acceptor based on barbituric acid (with R=H or R=Me), on cubic NLO properties of D-π-A ruthenium systems, using a constant donor. These derivatives were constructed using a *trans*-[Cl-Ru$(dppe)_2$(-C≡C)] (dppe = diphenylphosphinoethane) group as donor, and a *trans*-[CH=(pyrimidine-2,4,6-trione)] (R=H) barbituric acid group (complexes **a-c**) or a *trans*-[CH=(1,3-dimethylpyrimidine-2,4,6-trione)] (R=Me) N,N'-dimethylbarbituric group (complexes **a'-d'**) as acceptors. The colored complexes studied have been obtained in powder with modest to good efficiencies (see Table 1). Only the complex **d**, having for acceptor the barbituric acid (R=H) and for transmitter the thiophenyl-ene-thiophenyl group, could not be prepared for reasons too low solubility of the ligand.

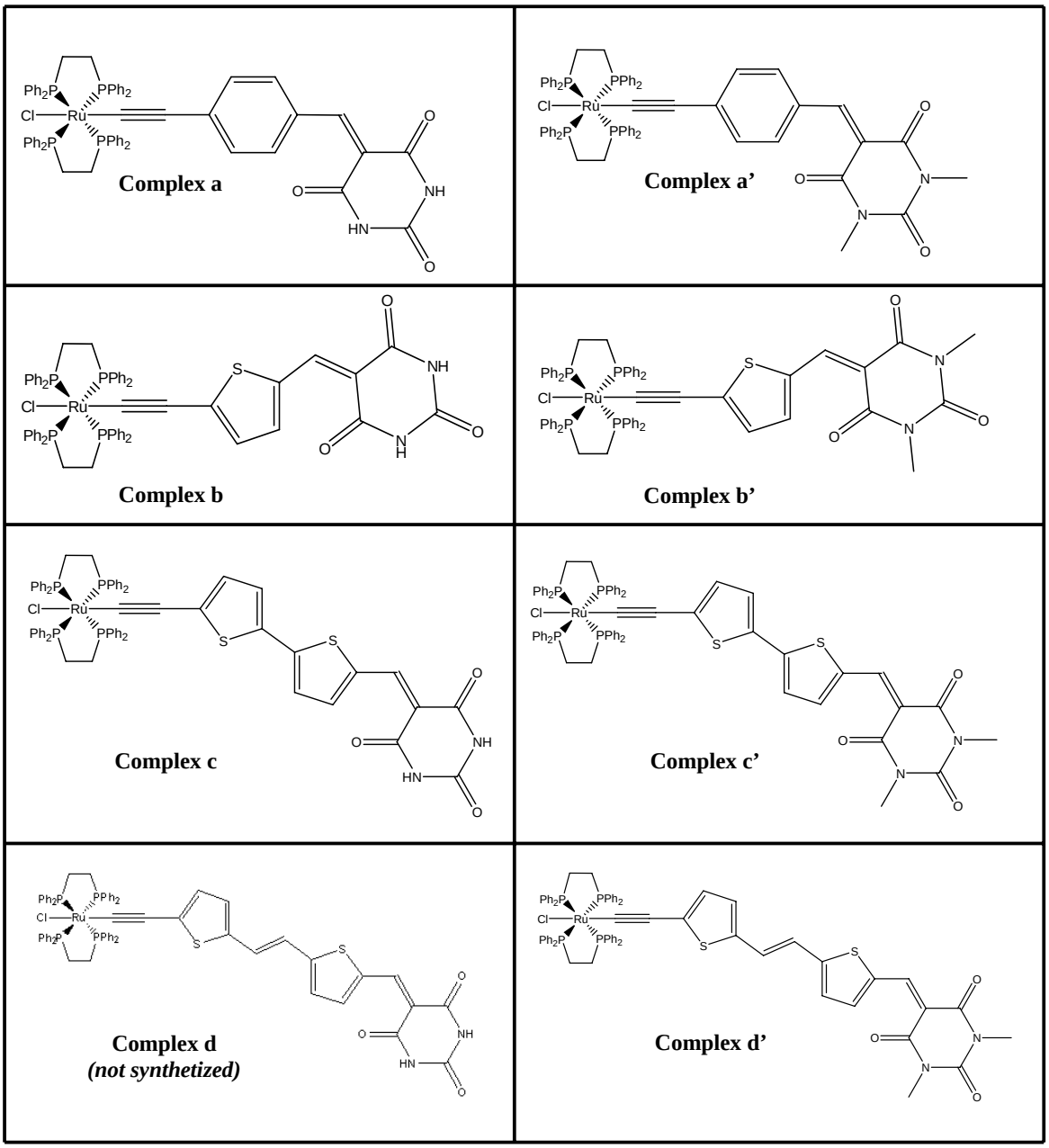


*Fig. 1. Chemical structures of studied complexes.*

*Table 1. Efficiency and color of each studied complex.*

| Complex | *Transmitter* | *R* | *Eff.* (%) | *Color* |
|---|---|---|---|---|
| **a** | p-phenyl | H | 76 | Dark blue |
| **a'** | p-phenyl | Me | 70 | Purple |
| **b** | 2,5-thiophenyl | H | 65 | Blue |
| **b'** | 2,5-thiophenyl | Me | 63 | Indigo |
| **c** | bithiophenyl | H | 66 | Dark green |
| **c'** | bithiophenyl | Me | 60 | Green |
| **d** | thiophenyl-ene-thiophenyl | H | *not synthetized* | |
| **d'** | thiophenyl-ene-thiophenyl | Me | 43 | Dark green |

**NMR and IR spectrocopy:** Table 2 presents the principal NMR and IR data of the studied complexes. The NMR spectra were recorded at 20 °C in deuterated chloroform $CDCl_3$ at 300, 121 and 75 MHz, for the proton $^1H$, phosphorus $^{31}P$ and carbon $^{13}C$, respectively. The IR spectra were recorded at 20 °C using pellets of potassium bromide KBr.

*Table 2. NMR and IR data of studied complexes.*

| Complex | $\nu_{Ru\text{-}C\equiv C}$ ($cm^{-1}$) | $\nu_{C=O}$ ($cm^{-1}$) | $\delta_{PPh_2}$ (ppm) | $\delta_C^{\alpha}$ (ppm) | $\delta_C^{\beta}$ (ppm) |
|---|---|---|---|---|---|
| **a** | 2038 | 1582 | 49.6 | 142.5 | 126.9 |
| **a'** | 2044 | 1598 | 50.0 | 151.5 | 126.9 |
| **b** | 2047 | 1599 | 48.5 | 148.1 | 116.7 |
| **b'** | 2012 | 1610 | 48.8 | 148.3 | 116.7 |
| **c** | 2019 | 1598 | 49.7 | *not soluble* | |
| **c'** | 2020 | 1588 | 49.8 | *not soluble* | |
| **d'** | 2014 | 1581 | 49.9 | *not soluble* | |

The NMR spectroscopy brings an additional information which confirms the proposed structures: in phosphorus NMR $^{31}P\{^1H\}$, we note the presence of a singulet signal towards 48-50 ppm, chemical shift very characteristic of the ruthenium complexes whose the metallic center $[RuCl(dppe)_2]$ is connected to a carbonated alkynyl ligand. The presence of singulets confirms the magnetic equivalence of the phosphorus atoms of the *dppe* groups and the *trans* position of chlorine ligand compared to the carbonated alkynyl ligand.

The complexes comprising a bithiophenyl transmitter (**c** and **c'**) or thiophenyl-ene-thiophenyl (**d'**) were too insoluble in deuterated solvents used to obtain their carbon $^{13}C$ NMR spectrum. The recorded spectra (phenyl or thiophenyl transmitter) present the characteristic signals of carbons α (Ru-C≡C) and β (Ru-C≡C) of alkynyl ligands, around 140-150 ppm for the first (**a** and **a'**) and 115-125 ppm for the second (**b** and **b'**).

In IR spectrometry, we observed very characteristic bands for the proposed structures: a fine and little intense band between 2010 and 2050 $cm^{-1}$ corresponding to the C≡C elongation of the alkynyl ligand connected to the ruthenium atom, and a fine and intense band between 1580 and 1610 $cm^{-1}$ corresponding to the C=O elongation of the carbonyl groups of the barbituric group.

**Cyclic voltammetry:** Within these complexes, the metallic ruthenium atom is at the oxidation number (II) and can be oxidized to the oxidation number (III). The corresponding oxidation potential depends naturally of the electronic density of the ruthenium atom which is function of the electronic contributions of different ligands. A comparison of the oxidation potentials of the studied complexes allows to evaluate the incidence of the acceptor (R=H or Me) and of the transmitter on the electronic richness of the metal, and thus, on the intramolecular electronic delocalization. The oxidation potentials were measured by means of cyclic voltammetry in dichloromethane solution (concentration close to $10^{-3}$ M). Electrochemical experiments were performed in a standard three-electrode system (platinum working/auxiliary electrodes and SCE reference electrode $E_{SCE/NEH}$ = 246 mV, NEH: Normal Electrode to Hydrogen) with $NBu_4PF_6$ (0.1 M) as the supporting electrolyte at 20 °C. Scan rates were typically 200 mV $s^{-1}$. A reversible process is observed in oxidation for the couple $Ru^{II}/Ru^{III}$ (see Fig. 2), characterized by a ratio of current $I_{PA}/I_{PC}$ close to the unit and by a difference of potential ΔE close to 65 mV.

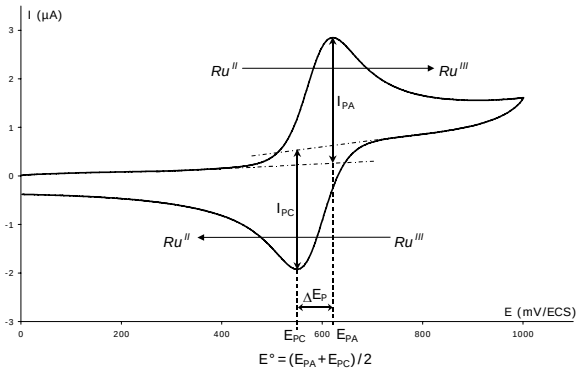


*Fig. 2. Voltamogramm obtained for the $Ru^{II}/Ru^{III}$ oxidation in the complex **b**.*

The transmitter which allows for obtaining the lower value of oxidation potential is the thiophenyl-ene-thiophenyl group (complex **d'**). Table 3 presents the standard potentials obtained for the different complexes. The long way of conjugation of transmitter on the one hand, the incidence of the electro-acceptor group on the electronic richness of metal to be minimized and allows, on the other hand, the charge of the oxidized form to be stabilized thanks to a better charge delocalization.

*Table 3. Electrochemical data of studied complexes.*

| Complex | $E^o$ (mV/SCE) | $\Delta E$ (mV) |
|---|---|---|
| **a** | 560 | 65 |
| **a'** | 530 | 70 |
| **b** | 615 | 65 |
| **b'** | 585 | 65 |
| **c** | 425 | 60 |
| **c'** | 390 | 70 |
| **d'** | 360 | 70 |

In addition, for each transmitter except the thiophenyl-ene-thiophenyl group (complex **d'**), we can compare the values obtained according to the used acceptor (R=H or R=Me). The complexes comprising the barbituric element (complexes **a-c**, R=H) have a potential

of oxidation higher than the methylated complexes (complexes **a'-c'**, R=Me). The intramolecular electronic metal → alkynyl transfert is more pronounced for a barbituric acceptor than for a N,N'-dimethylbarbituric acceptor: this last is less electroattractor.

**UV-VIS spectroscopy:** The UV-VIS absorption spectra of complexes **a-c** and **a'-d'** present several absorption bands (see Fig. 3).

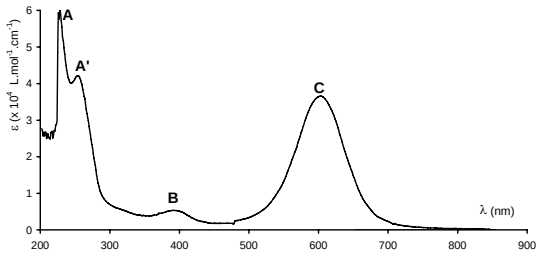


*Fig. 3. UV-VIS typical spectrum of a studied complex.*

The effects of the different transmitters and acceptors of the studied complexes on the absorption bands were evaluated by UV-VIS spectroscopy. The spectra were recorded at 20 °C in a dichloromethane solution (at the concentration $10^{-5}$ M) making it possible to respect the Beer-Lambert law. Table 4 presents the different data obtained. Each band of this spectrum can be allotted to one or more particular electronic transitions within complexes. The bands **A** and **A'**, situated in the UV part and having a low incidence on the color of the complexes, were allotted to electronic transitions of dppe diphosphine within the phenyl groups. The band **B**, with a lower molar extinction coefficient, is attributed to a transition of the π→π* (C≡C-Ar) intraligand charge transfer of the alkynyl, disturbed by the metal. Lastly, the band **C**, located at low energy and which determines the color of the complexes, is allotted to a transition $d_\pi$(Ru)→π* (C≡C-Ar) due to the metal-ligand charge transfer (MLCT).

*Table 4. Wavelengths λ (nm), numbers of wave $\bar{\nu}$ ($cm^{-1}$) and molar extinction coefficients ε (× $10^3$ $L.mol^{-1}.cm^{-1}$) of different bands of absorption spectra of studied complexes.*

| Complex | *A* | | | *A'* | | | *B* | | | *C* | | |
|---|---|---|---|---|---|---|---|---|---|---|---|---|
| | $\lambda_A$ | $\bar{\nu}_A$ | $\varepsilon_A$ | $\lambda_{A'}$ | $\bar{\nu}_{A'}$ | $\varepsilon_{A'}$ | $\lambda_B$ | $\bar{\nu}_B$ | $\varepsilon_B$ | $\lambda_C$ | $\bar{\nu}_C$ | $\varepsilon_C$ |
| **a** | 227 | 44050 | 84 | 254 | 39370 | 60 | 375 | 26670 | 12 | 588 | 17000 | 43 |
| **a'** | 228 | 43860 | 78 | 253 | 39530 | 63 | 363 | 27550 | 14 | 571 | 17510 | 48 |
| **b** | 227 | 44050 | 62 | 256 | 39060 | 42 | 397 | 25190 | 6 | 606 | 16500 | 36 |
| **b'** | 227 | 44050 | 67 | 255 | 39220 | 52 | 390 | 25640 | 9 | 593 | 16860 | 60 |
| **c** | 228 | 43860 | 62 | 252 | 39680 | 44 | 438 | 22830 | 11 | 681 | 14680 | 38 |
| **c'** | 228 | 43860 | 60 | 253 | 39530 | 43 | 429 | 23310 | 13 | 655 | 15270 | 35 |
| **d'** | 227 | 44050 | 65 | 252 | 39680 | 51 | 442 | 22620 | 16 | 672 | 14880 | 38 |

### 3. Degenerate four wave mixing technique

To interpret our experimental results, we used a model based on the coupled Maxwell nonlinear propagation equations [5, 48, 49] with taking into account linear absorption. The interacting waves are taken as plane waves $E^{<i>}(\vec{r},t)=A^{<i>}(\vec{r})e^{i(\vec{k}_i\vec{r}-\omega_i t)}+cc$ ($i$ = 1, 2, 3, 4) and using the slowly varying amplitude approximation, we obtain the DFWM efficiency as follows [5]:

$$R=\frac{I_4(0)}{I_3(0)}=\begin{cases}\dfrac{K^2}{\left[p.ctg(p.l)-\dfrac{\Psi}{2}\right]^2} & when\ \ \Psi^2-4K^2\le 0\\[2ex] \dfrac{K^2}{\left[q.ctgh(q.l)-\dfrac{\Psi}{2}\right]^2} & when\ \ \Psi^2-4K^2>0\end{cases} \quad (1)$$

where $p^2=K^2-(\Psi/2)^2$ ; $q=ip$ ; $\Psi=-(\Phi+\Phi^*)=-\alpha-2\beta(I_1(z)+I_2(z))$

and $K^2=\left(\dfrac{4\pi H}{nc}\right)^2(\chi'^2+\chi''^2)I_1(z)I_2(z)$ with: $\chi^{<3>}=\chi'+i\chi''$ ; $H=12\pi^2/n\lambda$ .

where $n$ is the linear refractive index of the material, $c$ the velocity of light propagation in vacuum, $l$ the cell length, $\lambda$ the wavelength of the laser, $\alpha$ the linear absorption coefficient, and $\beta$ the nonlinear absorption coefficient.

In the absence of nonlinear absorption, that means $\beta$ approach zero, the system (1) leads to the following formula:

$$R = \frac{I_4(0)}{I_3(0)} = \begin{cases} \dfrac{p^2 + \dfrac{\alpha^2}{4}}{\left[ p.ctg(p.l) + \dfrac{\alpha}{2} \right]^2} & when \quad p^2 \geq 0 \\ \dfrac{p^2 + \dfrac{\alpha^2}{4}}{\left[ q.ctgh(q.l) + \dfrac{\alpha}{2} \right]^2} & when \quad p^2 < 0 \end{cases} \tag{2}$$

where $p^2 = \left( \dfrac{48.\pi^3.\chi^{<3>}}{n^2.c.\lambda} \right)^2 . I_1^2 . e^{-\alpha.d} - \dfrac{\alpha^2}{4}$

and $q = ip$.

In the absence of linear and nonlinear absorption, that means $\alpha$ and $\beta$ approach zero, the system (1) leads to the following formula:

$$R = tg^2|p|l \tag{3}$$

where $p = \dfrac{48\pi^3}{n^2 c\lambda} \chi^{<3>} I_1(0)$.

We should notice here that the intensities are known experimentally, $\alpha$ and $\beta$ can be determined from the measurements of nonlinear transmission or UV-VIS spectra. Therefore the only parameter that remains to be determined is $\chi^{<3>}$. Taking into account linear and nonlinear absorption, the variation of the intensity of the pump waves along the *z*-axis may be expressed:

$$\frac{dI}{dz} = -(\alpha + \beta I)I \tag{4}$$

The transmission can be calculated from the following equation:

$$T = \frac{I(l)}{I(0)} = \frac{\alpha e^{(-\alpha l)}}{\alpha + \beta I(0)(1 - e^{-\alpha l})} \tag{5}$$

The best fit of Eq. (5) to experimental data allows us to deduce $\alpha$ and $\beta$ coefficients. Thus knowing the analytic formula of the DFWM efficiency $R$ (see Eq. (1-3)) and measuring the $I_4$ intensity, one can determine the value of $\chi^{<3>}$.

The geometry of the DFWM experimental setup is presented in Fig. 4. As a source of excitation we used 532 nm from a Q-switched mode locked Quantel Nd:YAG laser of 30 ps duration, and a repetition frequency of 1 Hz. First beam-splitter divide the beam to synchronize the acquisition from a fast photodiode. A glan prism (G) and a half-plate (λ/2) allow to modify the intensity of the laser beam. Second beam-splitter reflects about 6% of intensity (probe beam <3>). Non-reflected part of beam goes to next (third) beam splitter, which divides it in two pump beams <1> and <2>. Their intensities satisfy the relation $I_1(z=0) = I_2(z=l)$. The probe wave <3> is a weak probe beam $(I_3 = 10^{-2} I_1)$ which makes an angle of 12° with the direction of the two pump waves. The signal wave <4> is emitted in the opposite direction to the probe beam.

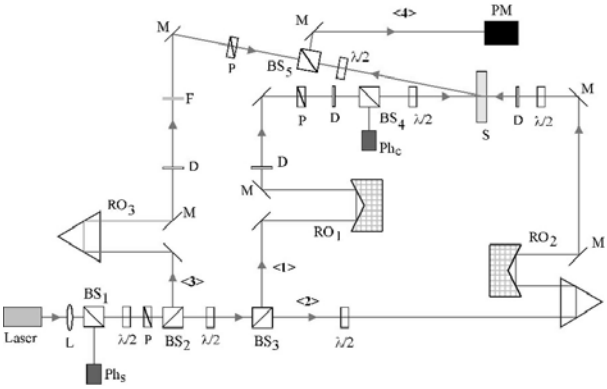


*Fig. 4. Experimental setup of DFWM: S - sample, RO - delay lines, G - glan prism, $Ph_s$, $Ph_c$ - synchronization and control photodiodes, BS - beam-splitters, PM - photomultiplier tube, <1> and <2> - pump waves, <3> - probe wave, <4> - fourth wave.*

In order to characterize an individual molecule, we determine the second-order hyperpolarizability using the following equation [50, 51]:

$$\chi^{<3>}_{solution} = \frac{N_A f_{solution} \rho_{solution}}{1 + C} \left[ \frac{\gamma_{solvent}}{M_{solvent}} + \frac{C\gamma}{M} \right] \tag{6}$$

with: $C = \dfrac{m}{m_{solvent}}$ ; $\rho_{solution} = \dfrac{m_{solution}}{V_{solution}}$ ;

$$f = (f_\omega)^3 f_{3\omega} \text{ and } f_{\omega,3\omega} = \frac{n^2_{\omega,3\omega} + 2}{3} \tag{7}$$

where $\gamma_{solvent}$ and $\gamma$ are the second-order optical hyperpolarizabilities of solvent (dichloromethane) and complex, respectively (in $m^5/V^2$), $f_\omega$ and $f_{3\omega}$ the Lorentz local field factor coefficients at fundamental and harmonic wavelengths, respectively (in our case $f_{solution} \approx f_{solvent}$), $N_A$ the Avogadro number, $M_{solvent}$ and $M$ the molecular masses of solvent and complex, respectively (in g/mol), and $C$ the ratio of masses of complex and solvent.

By replacing the relations (7) in the equation (6), we find a new expression:

$$\chi^{<3>}_{solution} = \frac{N_A f}{V_{solution}}\left(\frac{m_{solvent}\gamma_{solvent}}{M_{solvent}} + \frac{m\gamma}{M}\right) \quad (8)$$

For a highly diluted solution (i.e. when $C$ is close to 0), we obtain the expression giving the solvent third-order nonlinear optical susceptibility $\chi^{<3>}_{solvent}$ (in $m^2/V^2$):

$$\chi^{<3>}_{solvent} = \frac{N_A f \rho_{solvent}\gamma_{solvent}}{M_{solvent}} \quad (9)$$

In our case: $\rho_{solvent} = \rho_{CH_2Cl_2} = 1.32$ g/cm$^3$.

From equations (7) and (8), we obtain:

$$\chi^{<3>}_{solution} = \chi^{<3>}_{solvent} + \frac{N_A f \rho\gamma}{M} \quad (10)$$

Values reported in these SI units are related to commonly used *esu* units as $\chi^{<3>}_{(esu)} = (9\times10^8/4\pi)\,\chi^{<3>}_{(SI)}$. Second hyperpolarizability can be expressed in *esu* units as $\gamma_{(esu)} = (9\times10^{14}/4\pi)\,\gamma_{(SI)}$.

## 4. Theoretical simulations

For theoretical simulations of second-order hyperpolarizability, the six molecules **a-c'** were considered. Initially, geometry optimization (searching of the total energy minimum) for the molecule was performed. The $MM^+$ molecular force field method was used for total energy minimization and for building of the molecular optimized geometry [**52, 53**]. All quantum chemical calculations were performed by semi-empirical ZINDO/1 method within a framework of the restricted Hartree-Fock approach and convergence limit up to $10^{-6}$ eV after 500 iterations was achieved. The ZINDO/1 method is a modified version of the Intermediate Neglect of Differential Overlop (INDO), which is developed by Michael Zerner. Zerner's original INDO/1 used single and zeta Slater atomic orbital basis to calculate the wave functions and binding energies. The ZINDO/1 method was optimized as a universal semi-empirical method for calculating energy states in molecules containing transition metals (*3d* and *4d*).

The electronic spectra were calculated by the configuration interaction (CI) method with the maximum excitation energy up to 9 eV. Local perturbation were considered only within a framework of the isolated molecule. Therefore deviations from the experimental data will give information concerning the observed intramolecular and intermolecular interactions. The influence of the intermolecular electron vibration interactions is not taken into account. The values of second-order hyperpolarizability may be expressed in terms of the different energy levels from $g$ to $n$, of the molecule:

$$\gamma_{ijkl} = K\sum_{g=1}^{n}\frac{\left|\mu_i^{(g)}\right|\left|\mu_j^{g}\right|\left|M_k^{(g)} - M_k^{(0)}\right|\left|M_l^{(g)} - M_l^{(0)}\right|}{(E_g^2 - (2\hbar\omega)^2 + H)} \quad (11)$$

where $\mu_i^{(g)}, \mu_j^{(g)}$ are the transition dipole moment between the high occupied molecular orbital (HOMO) and the excited state, $\left|M_k^{(g)} - M_k^{(0)}\right|$ the difference between the excited (configuration interaction (CI) level) state dipole moment and ground state one, $E_g$ the transition energy from the ground to exited state, $\hbar\omega$ the energy of an incident laser photon, $H$ the line shape broadening, and $n$ the number of excited state.

Indices *i,j,k,l* = *x,y,z* are defined as laboratory Coordinate Cartesian system where *x*-axis corresponds to the longest axes of the molecule.

In this present work, we calculated only $\gamma_{xxxx}$, because the maximal output of nonlinear signal were observed usually for the diagonal tensor component, where the *x*-direction corresponds to polarizations direction of the laser beam (Fig. 6). The calculated values of the nonlinear optical hyperpolarizabilities are presented in the Table 9.

## 5. Results and discussion

For the studies of these complexes in solution, an increase of the concentration leads to an increase of the absorption, so we should find a compromise between optical nonlinearities and optical losses. For this purpose, we measured the influence of concentration on signal $I^{<4>}$ for each complex. We observed that all complexes display the same behaviour: a single maximum of $I^{<4>}$ that corresponds to an optimal value of concentration $C_{opt}$. Fig. 5 illustrates a typical example of these results for the complex **a**. One can observe that for concentrations larger than $C_{opt}$, the intensity of the signal decreases with an increase of concentration, which is due to the competition between the nonlinear mixing of the beams in interaction and the absorption growing with the concentration.

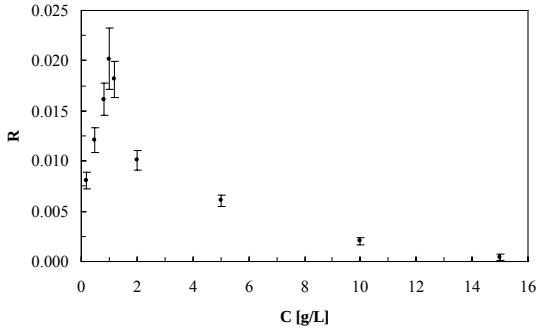


*Fig. 5. DFWM efficiency $R_{xxxx}$ versus concentration for the complex **a** ( $I^{<1>}$ = 1.0 GW/cm²) (in dichloromethane solvent).*

For each studied complex, the optimal value of molar concentration ($C_{opt}$ in mol/L) and the absorption coefficient ($\alpha$ in cm$^{-1}$) at $C_{opt}$ have been deduced from transmission measurements and in the range of used intensity (0 - 1.2 GW/cm²), and are collected in Table 5.

*Table 5. Parameters $M$, $C_{opt}$, $\lambda_{max}$, $T$ and $\alpha$ present the molar weight, optimal molar concentration, maximum absorption wavelength, transmission and linear absorption coefficients at $C_{opt}$, respectively.*

| Complex | $M$ [g mol$^{-1}$] | $C_{opt} \times 10^4$ [mol L$^{-1}$] | $\lambda_{max}$ [nm] | $T$ | $\alpha$ [cm$^{-1}$] |
|---|---|---|---|---|---|
| **a** | 1172.6 | 8.5 | 588 | 0.07 | 26.7 |
| **a'** | 1200.6 | 8.3 | 571 | 0.02 | 41.2 |
| **b** | 1178.6 | 8.5 | 606 | 0.11 | 22.0 |
| **b'** | 1206.6 | 8.3 | 593 | 0.03 | 36.6 |
| **c** | 1260.7 | 7.9 | 681 | 0.73 | 3.1 |
| **c'** | 1288.8 | 7.8 | 655 | 0.66 | 4.2 |
| **d'** | 1464.9 | 6.8 | 672 | 0.69 | 3.7 |
| $CS_2$ (ref.) | 76.1 | - | - | ~ 1 | ~ 0 |
| $CH_2Cl_2$ | 84.9 | - | - | ~ 1 | ~ 0 |

We have measured the efficiency $R$ at $C_{opt}$ as a function of the wave <1> intensity for different polarizations ($R_{xxxx}$, $R_{xxyy}$, $R_{yxyx}$, and $R_{yxxy}$) of incident beams. The studied solutions present the same behavior. Fig. 6 presents DFWM efficiency versus $I^{<1>}$ intensity for the complex **c**.

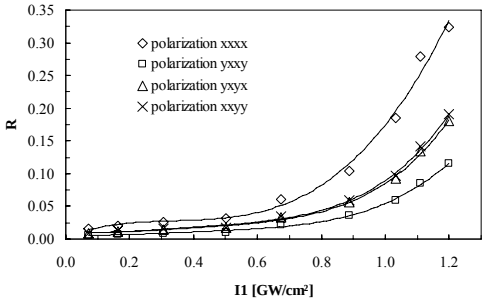


*Fig. 6. DFWM efficiency $R$ at $C_{opt}$ versus intensity $I^{<1>}$ for the complex **c** for different polarizations of incident beams (in dichloromethane solvent).*

We observe a good agreement between experimental results and the theoretical curve given by Eq. (6). The adjustment of the theoretical curve to experimental data allows us to estimate the third-order nonlinear optical susceptibility values $\chi^{<3>}$ for the studied complexes. The results are collected in Tables 6 and 7. Fig. 7 illustrates DFWM efficiency versus $I^{<1>}$ intensity of all complexes in vertical polarization of incident beams.

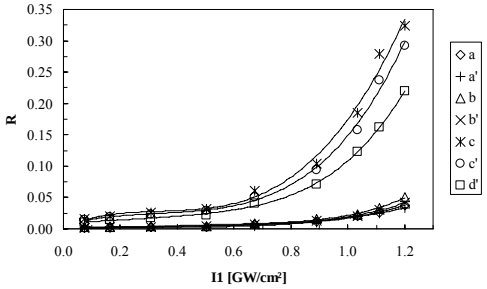


*Fig. 7. DFWM efficiency $R_{xxxx}$ at $C_{opt}$ versus intensity $I^{<1>}$ for studied complexes (in dichloromethane solvent).*

*Table 6. Parameters $\chi^{<3>}_{xxxx}$, $\chi^{<3>}_{xxyy}$, $\chi^{<3>}_{yxyx}$, $\chi^{<3>}_{yxxy}$, $\gamma_{xxxx}$ and $\chi^{<3>}_{xxxx}/\alpha$ present the third-order nonlinear susceptibilities for different polarizations of incident beams, the second-order nonlinear hyperpolarizability and the merit factor at $C_{opt}$, respectively (in dichloromethane solvent).*

| Complex | $\chi^{<3>}_{xxxx} \times 10^{20}$ [$m^2\ V^{-2}$] | $\chi^{<3>}_{xxyy} \times 10^{20}$ [$m^2\ V^{-2}$] | $\chi^{<3>}_{yxyx} \times 10^{20}$ [$m^2\ V^{-2}$] | $\chi^{<3>}_{yxxy} \times 10^{20}$ [$m^2\ V^{-2}$] | $\gamma_{xxxx} \times 10^{44}$ [$m^5\ V^{-2}$] | $\chi^{<3>}_{xxxx}/\alpha$ [arb. un.] |
|---|---|---|---|---|---|---|
| **A** | 0.34 | 0.13 | 0.23 | 1.21 | 0.16 | 0.01 |
| **A'** | 0.31 | 0.13 | 0.02 | 0.09 | 0.15 | 0.01 |
| **B** | 0.47 | 0.28 | 0.12 | 0.08 | 0.23 | 0.02 |
| **B'** | 0.39 | 0.26 | 0.12 | 0.07 | 0.19 | 0.01 |
| **C** | 3.01 | 1.79 | 0.27 | 0.16 | 1.56 | 0.97 |
| **c'** | 2.72 | 1.95 | 0.24 | 0.13 | 1.44 | 0.65 |
| **D'** | 2.04 | 0.98 | 1.77 | 1.07 | 1.23 | 0.55 |
| $CS_2$ (ref.) [**5**] | 1.94 | 0.24 | 1.94 | 1.01 | $4.71 \times 10^{-5}$ | - |
| $CH_2Cl_2$ | 0.15 | 0.03 | 0.97 | 0.68 | $3.95 \times 10^{-6}$ | - |

Taking advantage of different spatial symetries involved in the $\chi^{<3>}$ tensor, we can discrimine different physical mechanisms contributing to $\chi^{<3>}$. We have used a laser delivering pulses of 30 ps duration in our DFWM experiments, thus we can neglect thermal and electrostrictif effects which are slower. Two essential local effects contribute to the nonlinearities in isotropic media submitted to such laser pulses: deformations of electronic cloud and molecular (or nucleus) reorientation (translations, rotations and vibrations). Consequently, one can consider $\chi^{<3>}$ as being composed of two contributions corresponding to these mechanisms: $\chi^{<3>}_{ijkl} = \chi^{<3>el}_{ijkl} + \chi^{<3>m}_{ijkl}$. One can show that in isotropic media, the electronic and molecular contributions of tensorial components satisfy the following relations:

$$\chi^{<3>el}_{xxxx} = 3\chi^{<3>el}_{xxyy} = 3\chi^{<3>el}_{yxyx} = 3\chi^{<3>el}_{yxxy} \quad (12)$$

$$\chi^{<3>m}_{xxxx} = 8\chi^{<3>m}_{xxyy} = 8\chi^{<3>m}_{yxyx} = 4/3\,\chi^{<3>m}_{yxxy} \quad (13)$$

Notice that the following relationships are verified: for the $CS_2$ [49]:

$$\chi^{<3>\exp}_{xxxx} \approx 8.1\chi^{<3>\exp}_{xxyy} \approx 8.1\chi^{<3>\exp}_{yxyx} \approx 1.6\chi^{<3>\exp}_{yxxy} \quad (14)$$

for the $CH_2Cl_2$:

$$\chi^{<3>\exp}_{xxxx} \approx 5.0\chi^{<3>\exp}_{xxyy} \approx 5.0\chi^{<3>\exp}_{yxyx} \approx 1.7\chi^{<3>\exp}_{yxxy} \quad (15)$$

for the molecule a:

$$\chi^{<3>\exp}_{xxxx} \approx 2.6\chi^{<3>\exp}_{xxyy} \approx 2.6\chi^{<3>\exp}_{yxyx} \approx 4.3\chi^{<3>\exp}_{yxxy} \quad (16)$$

for the molecule a':

$$\chi^{<3>\exp}_{xxxx} \approx 2.4\chi^{<3>\exp}_{xxyy} \approx 2.4\chi^{<3>\exp}_{yxyx} \approx 4.2\chi^{<3>\exp}_{yxxy} \quad (17)$$

for the molecule b:

$$\chi^{<3>\exp}_{xxxx} \approx 1.7\chi^{<3>\exp}_{xxyy} \approx 1.7\chi^{<3>\exp}_{yxyx} \approx 3.0\chi^{<3>\exp}_{yxxy} \quad (18)$$

for the molecule b':

$$\chi^{<3>\exp}_{xxxx} \approx 1.5\chi^{<3>\exp}_{xxyy} \approx 1.5\chi^{<3>\exp}_{yxyx} \approx 3.0\chi^{<3>\exp}_{yxxy} \quad (19)$$

for the molecule c:

$$\chi^{<3>\exp}_{xxxx} \approx 1.7\chi^{<3>\exp}_{xxyy} \approx 1.7\chi^{<3>\exp}_{yxyx} \approx 2.8\chi^{<3>\exp}_{yxxy} \quad (20)$$

for the molecule c':

$$\chi^{<3>\exp}_{xxxx} \approx 1.4\chi^{<3>\exp}_{xxyy} \approx 1.4\chi^{<3>\exp}_{yxyx} \approx 2.7\chi^{<3>\exp}_{yxxy} \quad (21)$$

for the molecule d':

$$\chi^{<3>\exp}_{xxxx} \approx 2.1\chi^{<3>\exp}_{xxyy} \approx 2.1\chi^{<3>\exp}_{yxyx} \approx 3.0\chi^{<3>\exp}_{yxxy} \quad (22)$$

Experimental results described by Eq. (14-22) and the relations (12) and (13) allow us to deduce the results presented in Table 7.

*Table 7. The $\chi^{<3>}$ components deduced from the DFWM experiment for the studied complexes at $C_{opt}$ (in dichloromethane solvent).*

| Complex | $\chi^{<3>el}_{xxxx} \times 10^{20}$ [$m^2 V^{-2}$] | $\chi^{<3>m}_{xxxx} \times 10^{20}$ [$m^2 V^{-2}$] | $\lvert\chi^{<3>el}_{xxxx} / \chi^{<3>}_{xxxx}\rvert \times 10^{20}$ [$m^2 V^{-2}$] | $\lvert\chi^{<3>m}_{xxxx} / \chi^{<3>}_{xxxx}\rvert \times 10^{20}$ [$m^2 V^{-2}$] |
|---|---|---|---|---|
| **a** | 0.41 | -0.07 | 1.20 | 0.20 |
| **a'** | 0.38 | -0.07 | 1.23 | 0.23 |
| **b** | 0.66 | -0.19 | 1.41 | 0.41 |
| **b'** | 0.57 | -0.18 | 1.47 | 0.47 |
| **c** | 4.12 | -1.11 | 1.37 | 0.37 |
| **c'** | 4.21 | -1.49 | 1.55 | 0.55 |
| **d'** | 2.50 | -0.47 | 1.23 | 0.23 |
| $CS_2$ (ref.) [**5**] | 0.37 | 1.57 | 0.19 | 0.81 |
| $CH_2Cl_2$ | 0.04 | 0.11 | 0.25 | 0.75 |

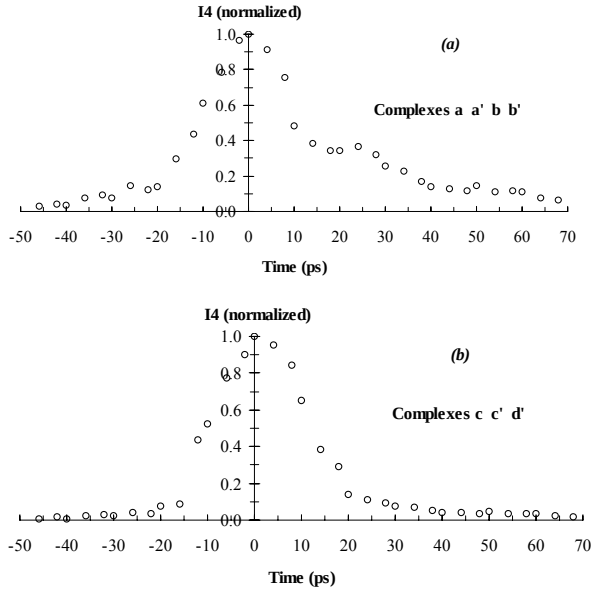


*Fig. 8. The intensity of the normalized signal $I^{<4>}$ of DFWM versus the delay time of the pump beam <2> (in dichloromethane solvent): (a) for complexes **a**, **a'**, **b**, **b'**, (b) for complexes **c**, **c'**, **d'**.*

The Fig. 8 presents the influence of the delay time of the second pump beam on the two others incident beams. From Fig. 8(a), one can observe the thermal effects and conclude that the linear absorption of these materials at 532 nm play substantial role on the third-order polarization. On the Fig. 8(b), thermal effects don't manisfest according to the weak absorption coefficients for the complexes **c**, **c'** and **d'**.

The results of the $\chi^{<3>}_{xxxx}$ values of studied complexes incorporated in PMMA matrices are also compared with the results in dicholoromethane solvent and presented in Table 8. The investigated samples were prepared as a mixture of 99.5% of PMMA and 0.5% of chromophore dissolved in 30 mL of tetrahydrofuran (THF) in the air atmosphere. The strongest values of $\chi^{<3>}_{xxxx}$ were obtained for the complexes incorporated in PMMA matrices and the smallest values were obtained for the complexes having the weakest quantity of double bonds and the shortest π-conjugated transmitters (complexes **a** and **b**).

*Table 8. Comparison of $\chi^{<3>}_{xxxx}$ parameter of studied complexes incorporated in dichloromethane solvent and PMMA matrix (chromophores concentration: 0.5%).*

| Complex | $\chi^{<3>}_{xxxx} \times 10^{20}$ [$m^2 V^{-2}$] in dichloromethane solvent | $\chi^{<3>}_{xxxx} \times 10^{20}$ [$m^2 V^{-2}$] in PMMA matrix |
|---|---|---|
| **a** | 0.34 | 3.43 |
| **a'** | 0.31 | 3.01 |
| **b** | 0.47 | 7.71 |
| **b'** | 0.39 | 6.08 |
| **c** | 3.01 | 60.50 |
| **c'** | 2.72 | 53.31 |
| **d'** | 2.04 | 39.17 |

In the Table 9 are presented the second-order hyperpolarizablility $\gamma^{exp}_{xxxx}$ deduced from the DFWM measurements and calculated $\gamma^{th}_{xxxx}$ from the quantum chemical simulations. Comparing the calculated and measured hyperpolarizabillity one can see smaller values of nonlinear optical coefficients $\gamma^{th}$ of calculated one. Actually the comparison the absolute values of theoretically calculated second-order hyperpolarizability with $\gamma^{exp}$ get from experiment can not bee made directly so we can compare the only trend of changes. However, the comparison calculated and measured hyperpolarizability is very interesting and may provide some information about intramolecular interactions.

One aim of the present work is the study of the influence of the small modifications in side group

(particularly methyl group) on the second-order nonlinear optical properties. From the theoretical calculations, we can conclude that the adjunction of methyl group to the end side group lead to the increase of nonlinear coefficient for compounds **b'** and **c'** except molecule **a'**. Received experimental results contrary to theoretical suggest that better nonlinear optical properties possess the compounds without added methylic groups. For the molecule **a** and **a'** the differences are small in limits of error.

*Table 9. Calculated and measured values of* $\gamma_{xxxx}$ *(*$\lambda = 532$ *nm).*

| Complex | $\gamma^{th}_{xxxx} \times 10^{49}$ [$m^5 V^{-2}$] for isolated molecule | $\gamma^{exp}_{xxxx} \times 10^{44}$ [$m^5 V^{-2}$] in dichloromethane solvent |
|---|---|---|
| **a** | 3.24 | 0.16 |
| **a'** | 3.17 | 0.15 |
| **b** | 0.77 | 0.23 |
| **b'** | 4.11 | 0.19 |
| **c** | 0.49 | 1.56 |
| **c'** | 11.51 | 1.44 |

The largest second-order hyperpolarizability measured for compounds **c** and **c'** is connected with the large electronic contribution to the observed results (see first column in Table 7). We can expect that for these two molecules **c** and **c'** including two thiophen rings in transmitter group, the intermolecular and vibration interactions play a key role in the observed nonlinearities what is not taken into account in suggested theoretical calculations. The smallest values of coefficient $\gamma^{exp}_{xxxx}$ obtained for molecules **a-b'** can be connected with the additional peaks on the Fig. 8(a) which presents the intensity $I^{<4>}$ of DFWM experiment versus time. For the complexes **a-b'**, it can indicate that we have a lot of excited trapping levels originating from highly-localized Ru $d$ states situating within the energy gap. As a consequence, the occupation of $d$-localized transition metal trapping levels should decrease. The appearance of additional number of trapping levels leads to occurrence of the larger number of the delocalized states within the energy gap [**54**]. We can conclude that described above effect is in general a deleterious effect on the $\chi^{<3>}$ properties for compound **a-b'** [**2**]. With this consideration, we can say that we have rather good agreement between the theoretical calculations and experimental data of second-order hyperpolarizability for all compounds. The greatest problem associated with nonlinear optical compounds is connected not only with ideal molecules but also at the incorporation of these molecules to form ideal macroscopic samples for nonlinear optics. The preparation of the samples is important in the obtained nonlinear optical properties of the samples, what can be the principal reason of disagreement between theoretical and experimental data.

## 6. Conclusions

A theoretical and experimental study of third-order nonlinear optical properties of alkynyl-ruthenium complexes bearing terminal hydrogen-bonding receptors has been presented. These materials could be promising materials for the molecular engineering for applications in organometallic chemistry and nonlinear optics. In this work, we have deduced the third-order nonlinear optical susceptibility $\chi^{<3>}$ for each studied complex. A good agreement between the proposed theoretical model and the experimental results was found. The investigated complexes show large optical nonlinearities in comparison with $CS_2$, which is the reference material for DFWM measurements.

We have shown that the complexes **c**, **c'** and **d'** have a weak absorption and so a strong merit factor ( $\chi^{<3>}_{xxxx} / \alpha$ ) compared to others complexes (**a**, **a'**, **b** and **b'**) and higher then the alkynyl-ruthenium derivatives studied previously [**2-4**]. We found, for all molecules studied in this work, that the electronic part of $\chi^{<3>}$ is dominant and its sign is positive. Moreover, the sign of molecular part of $\chi^{<3>}$ is negative. The maximally achieved value of $\chi^{<3>}$ in dichloromethane is obtained for complex **c** in vertical polarization of incident beams ( $\chi^{<3>}_{xxxx} = 3.0\times10^{-20}$ $m^2/V^2$) at 532 nm. The values of merit factors indicate that the complex **c**, which contains a bithiophenyl (R=H) transmitter, has the best third-order nonlinear optical properties. The second-order hyperpolarizabilities $\gamma$ of the studied molecules are about $10^4$ times greater than the hyperpolarizability of $CS_2$. These strong optical nonlinearities are due to the length of the $\pi$-conjugated system of the studied complexes (particularly for the complexes **c**, **c'** and **d'**). The results obtained show that the elongation of the transmitter and the termination of the acceptor group by a simple hydrogen bond lead to an increase of the microsocopic and macroscopic third-order nonlinear optical properties on these materials. Moreover, the complexes incorporated in PMMA matrices have a favorable influence on the $\chi^{<3>}$ values. Indeed, the maximally achieved value of $\chi^{<3>}$ in a PMMA matrix, obtained for complex **c** in vertical polarization of incident beams, is equal to: $\chi^{<3>}_{xxxx} = 60.5\times10^{-20}$ $m^2/V^2$ at 532 nm.

We have theoretically investigated contribution of the acceptor group to the output of the nonlinear coefficient for a new series of alkynyl ruthenium chromophores. The theoretical results for the molecule agree roughly with experimental data, taking into consideration a dispersion of the absorption fundamental edge caused by the intermolecular interactions. We have found that the reason

of disagreements on the optical properties between theoretical and experimental results is due to vibration and intermolecular contributions. The data thus obtained provide valuable insight into the origin of the hyperpolarizability and help to synthesize molecules with optimal properties which are important for nonlinear optics and molecular engineering.

## References


[1] S. Di Bella, Chem. Soc. Rev. **30**, 355-366 (2001).
[2] A. Migalska-Zalas, J. Luc, B. Sahraoui, I. V. Kityk, Opt. Mat. **28**, 1147-1151 (2006).
[3] A. Migalska-Zalas, B. Sahraoui, I. V. Kityk, S. Tkaczyk, V. Yuvshenko, J.-L. Fillaut, J. Perruchon, T. J. J. Muller, Phys. Rev. B, **79**, 0351191-0351198 (2005).
[4] J. Luc, J.-L. Fillaut, J. Niziol, B. Sahraoui, J. Optoelectron. Adv. Mater. **9**, 9, 2826-2832 (2007).
[5] B. Sahraoui, G. Rivoire, Opt. Comm. **138**, 109-112 (1997).
[6] G. Wilkinson, M. Rosenblum, M. C. Whiting, R. B. Woodward, J. Am. Chem. Soc. **74**, 2125-2126 (1952).
[7] D. Astruc, Chimie organométallique, EDP Sciences, Collection Grenoble Sciences (2000).
[8] S. Bai, F. Li, Q. Yang, H. M. Cheng, J. B. Bai, Chem. Phys. Lett. **376**(1-2), 83-89 (2003).
[9] A. Volger, H. Kunkely, Coord. Chem. Rev. **177**(1), 81-96 (1998).
[10] S. Barlow, S. R. Marder, Chem. Commun. **2000**, 1555-1562 (2000).
[11] P. G. Lacroix, Eur. J. Inorg. Chem. **2001**, 339-348 (2001).
[12] H. Le Bozec, T. Renouard, Eur. J. Inorg. Chem. **2000**, 229-239 (2000).
[13] C. E. Powell, M. G. Humphrey, Coord. Chem. Rev. **248**, 725-756 (2004).
[14] M. P. Cifuentes, M. G. Humphrey, J. Organomet. Chem. **689**, 3968-3981 (2004).
[15] M. I. Bruce, P. J. Low, K. Costuas, J.-F. Halet, S. P. Best, G. A. Heath, J. Am. Chem. Soc. **122**(9), 1949-1962 (2000).
[16] R. Dembinski, T. Bartik, B. Bartik, M. Jaeger, J. A. Gladysz, J. Am. Chem. Soc. **122**(5), 810-822 (2000).
[17] K.-T. Wong, J.-M. Lehn, S.-M. Peng, G.-H. Lee, Chem. Commun **2000**, 2259-2260 (2000).
[18] N. J. Long, C. K. Williams, Angew. Chem. Int. Ed. **2003**(42), 2586-2617 (2003).
[19] J. M. Tour, Acc. Chem. Res. **33**, 791-804 (2000).
[20] M. D. Ward, Chem. Soc. Rev. **34**, 121-134 (1995).
[21] K. Onitsuka, M. Fujimoto, N. Ohshiro, S. Takahashi, Angew. Chem. Int. Ed. Engl. **38**(5), 689-692 (1999).
[22] J. C. Calabrese, L.-T. Cheng, J. C. Green, S. R. Marder, W. Tam, J. Am. Chem. Soc. **113**(19), 7227-7232 (1991).
[23] J. L. Brédas, F. Meyers, B. M. Pierce, J. Zyss, J. Am. Chem. Soc. **114**(12), 4928-4929 (1992).
[24] I. Ledoux-Rak, J. Zyss, T. Le Bouder, O. Maury, A. Bondon, H. Le Bozec, J. Lumines. **111**, 307-314 (2005).
[25] K. Sénéchal, O. Maury, H. Le Bozec, I. Ledoux, J. Zyss, J. Am. Chem. Soc. **124**(17), 4560-4561 (2002).
[26] J. Zyss, I. Ledoux, Chem. Rev. **94**, 1, 77-105 (1994).
[27] B. J. Coe, Acc. Chem. Res. **39**(6), 383-393 (2006).
[28] S. Houbrechts, K. Clays, A. Persoons, V. Cadierno, M. Pilar Gamasa, J. Gimeno, Organometallics **15**(25), 5266-5268 (1996).
[29] Y. Umemura, A. Yamagishi, R. Schoonheydt, A. Persoons, F. De Schryver, J. Am. Chem. Soc. **124**(6), 992-997 (2002).
[30] P. Yuan, J. Yin, G. Yu, Q. Hu, S. Hua Liu, Organometallics, **26**(1), 196-200 (2007).
[31] B. J. Coe, S. Houbrechts, I. Asselberghs, A. Persoons, Angew. Chem. Int. Ed., **38**(3), 366-369 (1999).
[32] H. Sakaguchi, L. A. Gomez-Jahn, M. Prichard, T. L. Penner, D. G. Whitten, T. Nagamura, J. Phys. Chem. **97**(8), 1474-1476 (1993).
[33] A. M. McDonagh, M. G. Humphrey, M. Samoc, B. Luther-Davies, S. Houbrechts, T. Wada, H. Sasabe, A. Persoons, J. Am. Chem. Soc. **121**(6), 1405-1406 (1999).
[34] D. M. Burland, R. D. Miller, C. A. Walsh, Chem. Rev. **94**(1), 31-75 (1994).
[35] D. S. Chemla, J. Zyss, Nonlinear Optical Properties of Organic Molecules and Crystals, Academic Press, Orlando, FL (1987).
[36] I. R. Whittall, M. G. Humphrey, M. Samoc, J. Swiatkiewicz, B. Luther-Davies, Organometallics **14**(12), 5493-5495 (1995).
[37] S. K. Hurst, M. P. Cifuentes, A. M. McDonagh, M. G. Humphrey, M. Samoc, B. Luther-Davies, I. Asselberghs, A. Persoons, J. Organomet. Chem. **642**(1-2), 259-267 (2002).
[38] C. E. Powell, M. P. Cifuentes, J. P. Morrall, R. Stranger, M. G. Humphrey, M. Samoc, B. Luther-Davies, G. A. Heath, J. Am. Chem. Soc. **125**(2), 602-610 (2003).
[39] S. K. Hurst, M. P. Cifuentes, J. P. L. Morrall, N. T. Lucas, I. R. Whittall, M. G. Humphrey, I. Asselberghs, A. Persoons, M. Samoc, B. Luther-Davies, A. C. Willis, Organometallics **20**, 4664-4675 (2001).
[40] P. C. Jayprakash, R. I. Matsuoka, M. M. Bhadbhade, V. G. Puranik, P. K. Das, H. Nishihara, A. Sarkar, Organometallics **18**(19), 3851-3858 (1999).
[41] C. Lebreton, D. Touchard, L. Le Pichon, A. Daridor, L. Toupet, P. H. Dixneuf, Inorg. Chim. Acta, **272**, 188-196 (1998).
[42] I. R. Whittall, M. G. Humphrey, D. C. R. Hockjless, B. W. Skelton, A. H. White, Organometallics **14**(8), 3970-3979 (1995).
[43] J.-L. Fillaut, J. Andriès, L. Toupet, J-P. Desvergne, Chem. Comm. **2005**, 2924-2926 (2005).
[44] J.-L. Fillaut, M. Price, A. L. Johnson, J. Perruchon, Chem. Comm. **2001**, 739-740 (2001).
[45] J.-L. Fillaut, J. Andriès, J. Perruchon, Inorg. Chem. Comm. **5**(12), 1048-1051 (2002).
[46] T. Gustavsson, L. Cassara, V. Gulbinas, G.

Gurzadyan, J.-C. Mialocq, S. Pommeret, M. Sorgius, P. Van Der Meulen, J. Phys. Chem. A, **102**(23), 4229-4245 (1998).
[47] J.-L. Fillaut, J. Andriès, J. Perruchon, J.-P. Desvergne, L. Toupet, L. Fadel, B. Zouchoune, J.-Y. Saillard, Inorg. Chem. **46**(15), 5922-5932 (2007).
[48] R. W. Boyd, Nonlinear Optics, Academic Press, New York (1992).
[49] B. Sahraoui, M. Sylla, J. P. Bourdin, G. Rivoire, J. Zaremba, J. Modern Opt. **42**(10), 2095-2107 (1995).
[50] F. Kajzar, I. Ledoux, J. Zyss, Phys. Rev. A, **36**(5), 2210-2219 (1987).
[51] P. N. Prasad, Nonlinear optical effects in organic materials, Contemporary nonlinear optics, Academic Press Inc., 265 (1992).
[52] S. J. Weiner, P. A. Kollman, D. A. Case, U. C. Ghio, G. Alagona, J. S. Profeta, P. Weiner, J. Am. Chem. Soc. **106** (3), 765-784 (1984).
[53] S. J. Weiner, P. A. Kollman, D. T. Nguyen, D. A. Case, J. Comput. Chem. **7**(2), 230-252 (1986).
[54] A. Migalska-Zalas, Z. Sofiani, B. Sahraoui, I. V. Kityk, S. Tkaczyk, V. Yuvshenko, J.-L. Fillaut, J. Perruchon, T. J. J. Muller. J. Phys. Chem. B, **108**(39), 14942-14947 (2004).

*Corresponding author: bouchta.sahraoui@univ-angers.fr